

Electronic Supplementary Information (ESI)

A sustainable lecithin-based ligand for the bio-functionalization of iron and hybrid metal organic frameworks (MOFs) nanoparticles with the sugar mannose

Camilla M. Cova,^a Víctor Ramos,^a Alberto Escudero,^{a,b} Juan P. Holgado,^c Nouredine Khier*^a and Alessio Zuliani*^a

^a Asymmetric Synthesis and Functional Nanosystems Group (Art&Fun), Institute for Chemical Research (IIQ), CSIC-University of Seville, 41092 Sevilla, Spain

^b Department of Inorganic Chemistry, Faculty of Chemistry, University of Seville, 41012 Sevilla, Spain

^c Instituto de Ciencia de Materiales and Departamento de Química Inorgánica, CSIC-University of Seville, 41092 Sevilla, Spain

*Corresponding author: a.zuliani@csic.es; khier@iiq.csic.es

Table of contents

S1. Materials and characterization techniques	2
1.1. Materials	2
1.2 Characterization	2
S2. Methods.....	3
2.1 Details for the synthesis of the ligand.....	3
2.2 Synthesis of PCN-222	3
2.3 Synthesis of MIL-101 (Fe).....	3
2.4 Synthesis of UiO-66	3
2.5 Synthesis of iron particles (akageneite)	4
2.6. Functionalization of nanostructures	4
S3. Probability of double bonds in phosphatidylcholine	4
S4. HPLC and Mass spectroscopy analysis	5
S5. Elemental analysis	8
S6. Nuclear magnetic resonance (NMR) analysis (SI)	9
S7. Green metrics values	15
S8 Raman spectrometry	16
S9. DLS analysis.....	17
S10. SEM images with mapping.....	18
S11. XPS analysis.....	19
References.....	20

S1. Materials and characterization techniques

1.1. Materials

L- α -phosphatidylcholine, soybean (14-29 wt% choline basis, 13 wt% C16:0 (palmitic), 4 wt% C18:0 (stearic), 10 wt% C18:1(oleic), 64 wt% C18:2 (linoleic), and 6% 18:3 (linolenic)), L-Cysteine (anhydrous, $\geq 99.0\%$), 2,2-dimethoxy-2-phenylacetophenone (DMPA) (99%), D-mannose ($\geq 99\%$), Zr(OBu)₄ in n-butanol (80 wt%), benzoic acid (ACS reagent, $\geq 99.5\%$), isopropanol (iPrOH, natural, $\geq 98\%$), ethanol (EtOH, 96%, EMPROVE[®] EXPERT, Ph. Eur., BP, ChP), N,N-dimethylformamide (DMF; anhydrous, 99.8%), trifluoroacetic acid (TFA, ReagentPlus[®], 99%), dimethyl sulfoxide (DMSO, $\geq 99\%$), acetic acid (glacial $\geq 99\%$), terephthalic acid (98%), ZrCl₄ ($\geq 99.5\%$), triethylamine ($\geq 99.5\%$), FeCl₃·6H₂O (99%), methanol (96%), and chloroform-d (99.8 atom %D) were purchased from Merck KGaA (Darmstadt, Germany). Tetrakis(4-carboxyphenyl)porphyrin (TCPP) (97%) was purchased from BLD Pharmatech Ltd (Shanghai, China). All the chemicals were used without any further purification.

1.2 Characterization

Fourier-Transform Infrared Spectroscopy (FTIR) analysis was performed with a Bruker Tensor 27 spectrophotometer using an ATR cell. Spectra were recorded at room temperature in the range of 400 to 4000 cm⁻¹ with a resolution of 2 cm⁻¹. Dynamic Light Scattering (DLS) measurements were performed using a Malvern Zetasizer Nano ZSP equipped with a 10 mW He-Ne laser operating at a wavelength of 633 nm and fixed scattering angle of 173°. Diluted samples (ca. 0.2 mg mL⁻¹) were loaded into a quartz cuvette, and then three measurements, each consisting of ten data runs, were taken at room temperature after an equilibrating run of 30 sec. Scanning Electron Microscopy (SEM) images were acquired using a HITACHI S4800 field emission microscope equipped with Energy-dispersive X-ray spectroscopy (EDX) operating at 2 kV in secondary electron and backscattered electron modes. The samples were prepared by drying a diluted dispersion of the particles on a silicon wafer substrate under ambient conditions. ¹³CNMR and ³¹PNMR spectra were recorded on a 600 MHz Bruker Avance III HD spectrometer (14.09 T) and Bruker AVHD 500 MHz (11.74 T) and referenced to residual solvent peaks. Peak positions are given in ppm. Mass spectrometry (MS) were performed with a high-resolution Q-Exactive hybrid quadrupole orbitrap mass spectrometer from Thermo Scientific. ICP-OES analysis was performed using a ThermoFisher Scientific iCAP 7200 ICP-OES Duo. Prior to analysis, samples were treated by microwave-assisted digestion with aqua regia (3:1 nitric acid to hydrochloric acid). Elemental Analysis were performed using an Elemental Analyzer LECO TruSpec CHNS. Raman analysis were performed using a Horiba Jobin Yvon LabRAM HR Raman spectrometer using 532 nm laser excitation. XPS analyses were carried out by using a SPECS Phoibos 150 instrument using a non-monochromatic Al K alpha X-ray source (20 mA, 14 kV). The instrument BE energy scale (work function) was calibrated to give a binding energy (BE) at 83.96 eV for the Au 4f_{7/2} signal for freshly ion etched metallic gold (Au). The spectrometer dispersion (energy range) was adjusted to give a BE at 932.62 eV for the Cu 2p_{3/2} line of freshly ion etched metallic copper (Cu). The charge compensation (neutralizer) system was used on all non-conductive specimen samples. The surface of each non-conductive sample was irradiated with a flood of electrons accelerated to 2.0-4.0 eV to produce a nearly neutral surface charge. Survey scan analyses (0-1100 eV range) were carried out by using a pass energy of 50 eV. High energy resolution chemical state analyses (20-50 eV wide range) were carried out by using a pass energy of 20 eV. Data from all insulating materials have been charge corrected (referenced) using the main signal of the Ti2p_{3/2} at ca. 458.6 eV, double checking that with this calibration adventitious carbon C1s spectrum (hydrocarbon, C-C, moiety) peaks at 284.6±0.1 eV. Measurement of angular rotation ([α]) was performed operating at 20 °C on a Jasco P-2000 polarimeter (Tokyo, Japan) equipped with a deuterium lamp (589 nm). Samples were used at a concentration of 10 mg ml⁻¹. Prior to analysis, the calibration of the instrument was verified using D-mannose, obtaining [α]_D²⁰ = 13.71°.

52. Methods

2.1 Details for the synthesis of the ligand

The ligand was firstly prepared by reacting phosphatidylcholine with cysteine. To dissolve lecithin in EtOH, the mixture can be slightly heated if necessary ($< 50\text{ }^{\circ}\text{C}$ for a short time, generally less than 10 minutes), and then naturally cooled down to r.t.. Concerning the photo-“click” reaction, it can be performed using a UV lamp used to reveal TLC. The lamp can be vertically placed near to a stirring plate, where the mixture of the different components is placed in a proper vessel, *i.e.*, a vessel not adsorbing UV-radiation. IMPORTANTLY, the lamp and the reaction mixture must be completely covered to block UV-radiation. The reaction was repeated five times. One time, after the photo “click”-reaction, and with the scope of performing mass spectroscopy, the crude product was purified by chromatographic column using a mixture of dichloromethane and methanol (10:1) as the eluent and **Phos-Cys** product was obtained as confirmed by mass spectroscopy. The reactor and employed tool were cleaned with 15 mL of EtOH. Regarding the c.f. synthesis, prior to the reaction, the reactor was washed with EtOH (0.3 mL min^{-1} flow, 30 minutes). Sequentially, the reaction solution was pumped through and the reaction conditions were optimized based on previous studies with similar substrates.¹ The reaction was repeated five times, and in one case, after the reaction, the crude product was purified by chromatographic column using a mixture of dichloromethane and methanol (10:1) as the eluent and **Phos-Cys-Man** product (10 g) was obtained as confirmed by mass spectroscopy. The reactor was washed with ethanol (0.5 mL min^{-1} flow, 12 minutes). Tools used for the synthesis were cleaned with 5 mL ethanol.

2.2 Synthesis of PCN-222

Zr₆ nodes/clusters were prepared as follow: operating under argon atmosphere, 15 mL of 80 wt% Zr(OBu)₄ (32.5 mmol, MW 383.67 g mol⁻¹) in n-butanol and 100 g of benzoic acid (0.82 mol, MW 122.12 g mol⁻¹) were added to 300 mL of isopropanol (iPrOH) or 300 mL of n-propanol. Sequentially, the mixture was heated under reflux with stirring overnight. The excess of solvent was removed by vacuum heating, leading to the formation of a white solid powder. The solid was extensively washed with iPrOH and then dried under vacuum at room temperature. PCN-222 was prepared based on a previously reported method.² In details, 30 mg TCPP (0.0379 mmol, MW 790.77 g mol⁻¹), 45 mg Zr₆ cluster (0.038 mmol, MW 1164 g mol⁻¹), and 150 μL TFA (1.95 mmol) were dissolved in 10 mL of DMSO in a 10 mL sealed vial. The resulting mixture was heated at $120\text{ }^{\circ}\text{C}$ for 24 hours under no mixing and then allowed to cool down to room temperature. The dark, purple-coloured MOF was collected by high-speed centrifugation (12 000 rpm, 15 min), washed one time with DMSO, and exchanged two times with methanol (MeOH).

2.3 Synthesis of MIL-101 (Fe)

For the synthesis of MIL-101(Fe), 1.73 g of FeCl₃·6H₂O (6.40 mmol, MW 270.32 g mol⁻¹) were dissolved in 10 mL DMF to obtain a 0.64 M solution. Parallely, 530 mg of terephthalic acid (3.19 mmol, MW 166.13 g mol⁻¹) were dissolved in 10 mL of DMF to prepare a 0.32 M solution. The two solutions were thus mixed with 130 mL of DMF and with 6 mL of acetic acid. The mixture was heated 120°C for 24 hours. After cooling down to room temperature, the MOF was collected by high-speed centrifugation (7 000 rpm, 15 min), washed one time with DMF, and exchanged two times with MeOH.

2.4 Synthesis of UiO-66

UiO-66 was prepared by dissolving 0.312 g of ZrCl₄ (1.34 mmol, MW 233.04 g mol⁻¹) in 40 mL DMF.³ Parallely, 1 g of terephthalic acid (6.02 mmol, MW 166.13 g mol⁻¹) was dissolved in 40 mL DMF. Then, the Zr-solution was added to the terephthalic acid solution. Finally, 40 mL of acetic acid was added slowly under stirring conditions. The mixture was stirred under reflux for 24 h at $120\text{ }^{\circ}\text{C}$. UiO-66 was collected by high-speed centrifugation (7000 rpm, 15 min), washed one time with DMF, and exchanged two times with MeOH.

2.5 Synthesis of iron particles (*akageneite*)

3.4 g of $\text{FeCl}_3 \cdot 6\text{H}_2\text{O}$ (12.58 mmol, MW 270.32 g mol⁻¹) was dissolved in 340 mL water at 90 °C under reflux.⁴ Sequentially 0.1 mL of glacial acetic acid was added. The mixture was thus heated under stirring at 90 °C for 1 hour. The so obtained brownish solid was filtrated and washed with water, thus collected and redispersed in MeOH.

2.6. Functionalization of nanostructures

The functionalization of the nanostructures was carried out by dissolving 150 mg of **Phos-Cys-Man** ligand (0.14 mmol, MW *ca.* 1068 g mol⁻¹) in 5 mL milli-Q H₂O. This solution was added to 15 mg of each nanostructure. Each mixture was kept at 60°C for 24 hours. After that, each solution was centrifuged at 5000 rpm for 15 minutes. Each sample was then washed two times with water and one time with ethanol and centrifuged again under the same conditions. Finally, the functionalized NPs were redispersed in MeOH or dried for characterization.

5.3. Probability of double bonds in phosphatidylcholine

Commercially available phosphatidylcholine was composed of 13 wt% C16:0, 4 wt% C18:0, 10 wt% C18:1, 64 wt% C18:2, and 6 wt% 18:3, thus a total of 83 wt% of fatty acid chains present at least one double bond. Since phosphatidylcholine is composed of two chains *per* molecules, two steps are needed to calculate the probability that at least one of the chains present at least one double bond. The probability of having one chain without any double bond is:

$$P = \frac{17}{100}$$

Then, the probability of having a second chain without any double bond is:

$$P = \frac{16}{99}$$

The two joint probabilities combined together are:

$$P = \frac{17}{100} \cdot \frac{16}{99} = 2.75\%$$

Thus, the probability of having at least one chain presenting at least one double bond is 97.25%.

S4. HPLC and Mass spectroscopy analysis

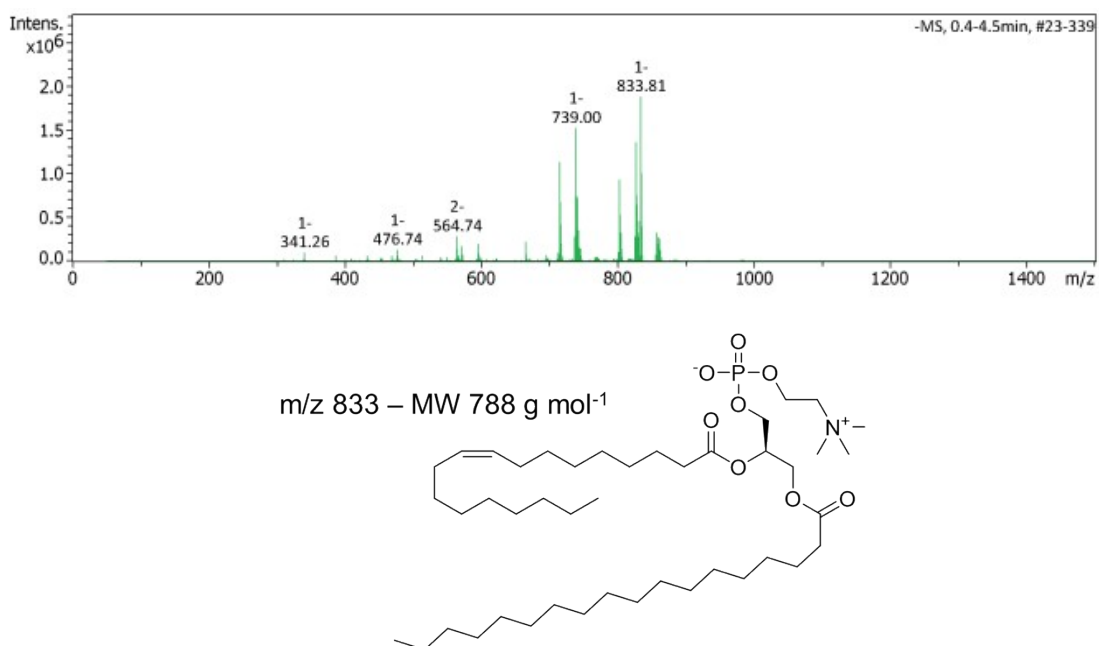


Fig. S1. Spectrum of phosphatidylcholine using mass spectrometry and structure of the phosphatidylcholine.

Table S1. Peaks of mass spectrometry of phosphatidylcholine.

m/z	z	I
715.19	1-	113418
		4
716.12	1-	677195
717.04	1-	421889
739.00	1-	151486
		2
739.87	1-	747385
740.85	1-	721610
741.84	1-	310488
742.88	1--	364153
802.99	1-	
		932285
803.87	1-	529793
804.85	1-	333050
826.97	1-	135948
		8
827.70	1-	756100
828.62	1-	649017
830.86	1-	332024
831.96		646680
		6
833.81	1-	187894
		3
834.55	1-	100525
		1
835.56	1-	402457
857.72	1-	332523

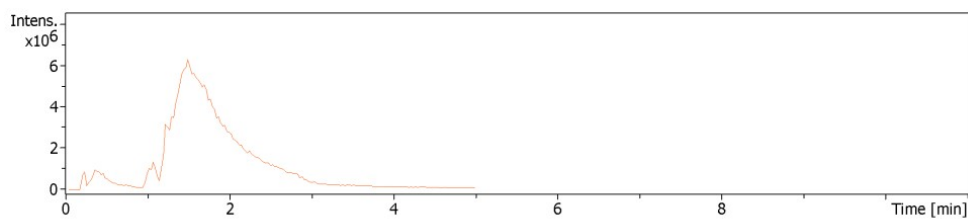


Fig. S2. Spectrum of **Phos-Cys** using HPLC.

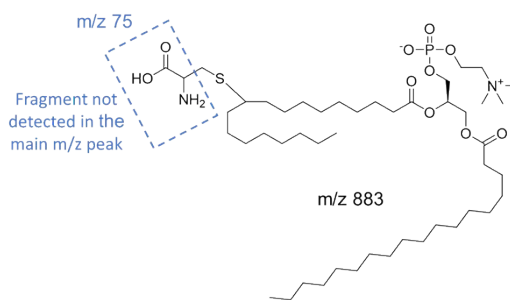
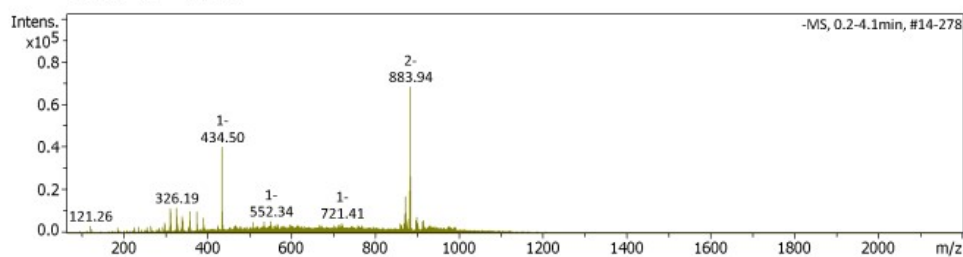


Fig. S3. Spectrum of **Phos-Cys** using mass spectrometry and structure of the **Phos-Cys** (Chemical Formula: $C_{47}H_{93}N_2O_{10}PS$).

Table S2. Peaks of mass spectrometry of **Phos-Cys**.

m/z	z	I
312.12		11544
312.69	1-	9615
326.19		11816
326.76	1-	10908
327.33	2-	7706
358.26	2-	10094
374.46	2-	9850
434.50	1-	40168
435.03	2-	24258
435.92	2-	9831
871.18	2-	7728
871.86	2-	8750
872.62	1-	17062
873.62	1-	9379
882.71		19832
883.21		11255
883.94	2-	68053
884.48	2-	44663
885.05	2-	26379

885.77 2- 15639

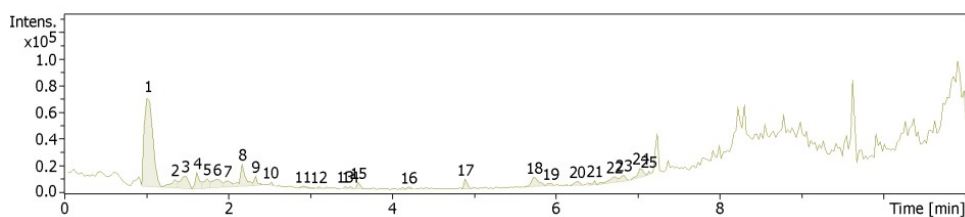


Fig. S4. Spectrum of Phos-Cys-Man using HPLC.

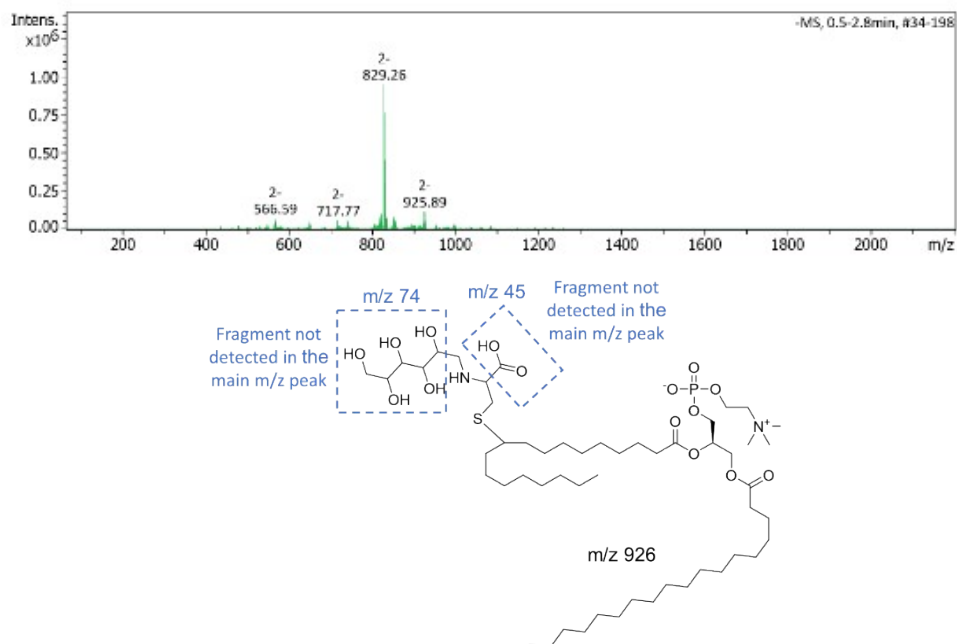


Fig. S5 Spectrum of Phos-Cys-Man using mass spectrometry and structure of the Phos-Cys-Man (Chemical Formula: $C_{53}H_{105}N_2O_{15}PS$).

Table S3. Peaks of mass spectrometry of Phos-Cys-Man.

m/z	z	I
566.59	2-	72014
819.50	2-	78977
822.07	2-	100764
822.77	2-	93240
823.46	1-	101671
828.62	2-	923995
829.26	2-	948499
829.86	2-	764075
830.40	2-	437467
831.07	2-	456472
831.62	2-	257498
832.25	1-	307603
832.84	2-	92654
833.42	1-	106124
834.42	1-	78325
852.25	2-	75601
852.99	2-	83205
853.60	2-	71261

925.89 2- 119557
 927.13 2- 115377

S5. Elemental analysis

Table S4. Results of the CHNS% analysis.

wt%	Phosphatidylcoline			Phos-Cys			Phos-Cys-Man		
	Theor.	Exp. 1	Exp. 2	Theor.	Exp. 1	Exp. 2	Theor.	Exp. 1	Exp. 2
C	67.5	60.2	60.1	62.5	51.9	52.0	59.6	40.5	41.1
H	10.4	8.8	9.0	9.4	8.9	8.5	9.4	7.5	7.3
N	1.8	1.0	1.2	3.1	3.2	3.6	3.1	1.0	0.8
S	0.0	0.3	0.2	3.5	5.7	5.7	2.9	1.9	1.4

S6. Nuclear magnetic resonance (NMR) analysis (SI)

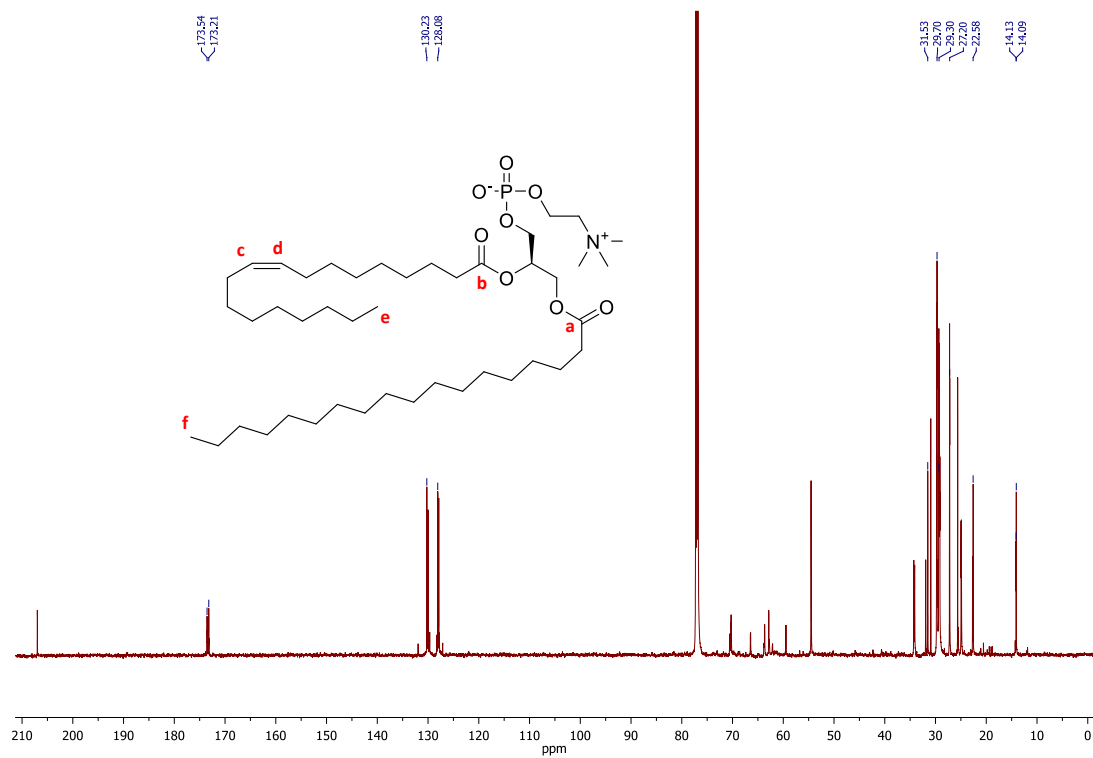


Fig. S6. ¹³C NMR spectrum of phosphatidylcholine.

¹³C NMR (150 MHz, CDCl₃, 25°C) phosphatidylcholine: δ 173.5 and 173.2 (–COO– **a** and **b**), 130.2 and 128.1 (–CH=CH– **c** and **d**), 31.5, 29.7, 29.3, 27.2, 22.5, and others (several –CH₂– methylene groups), 14.1 (two terminal –CH₃ **e** and **f**). Residual acetone peaks δ 207 and 31 ppm, and dichloromethane 54 ppm.

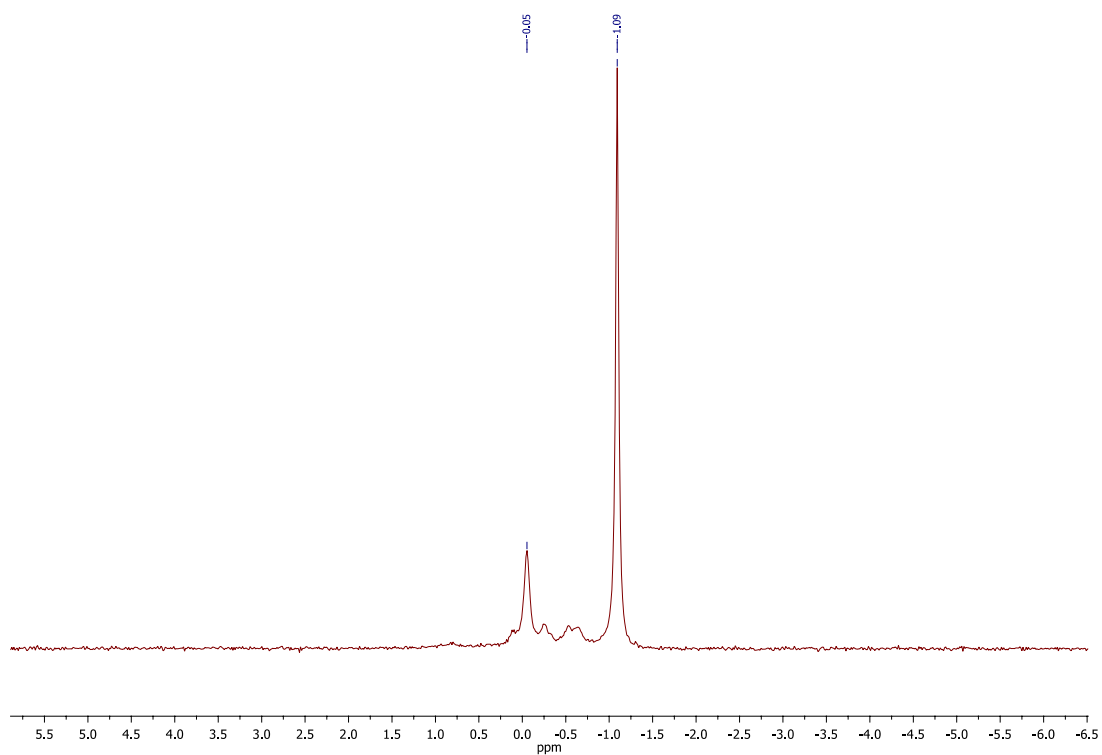


Fig. S7. ^{31}P NMR spectrum of phosphatidylcholine.

^{31}P NMR (173 MHz, CDCl_3 , 25°C) phosphatidylcholine: δ -1.09 s, and -0.05 s ppm. Smaller peaks at -0.2 and -0.6 ppm. It should be taken into account that the phosphatidylcholine is a natural and not fully purified product, and that the presence of small amounts of other phospholipids with similar structures, or with different ligands (Fig. 3 in the main text), cannot be excluded. Thus lower intensity ^{31}P signals can appear on the ^{31}P spectrum, compared to the unique P environment expected for a pure compound.

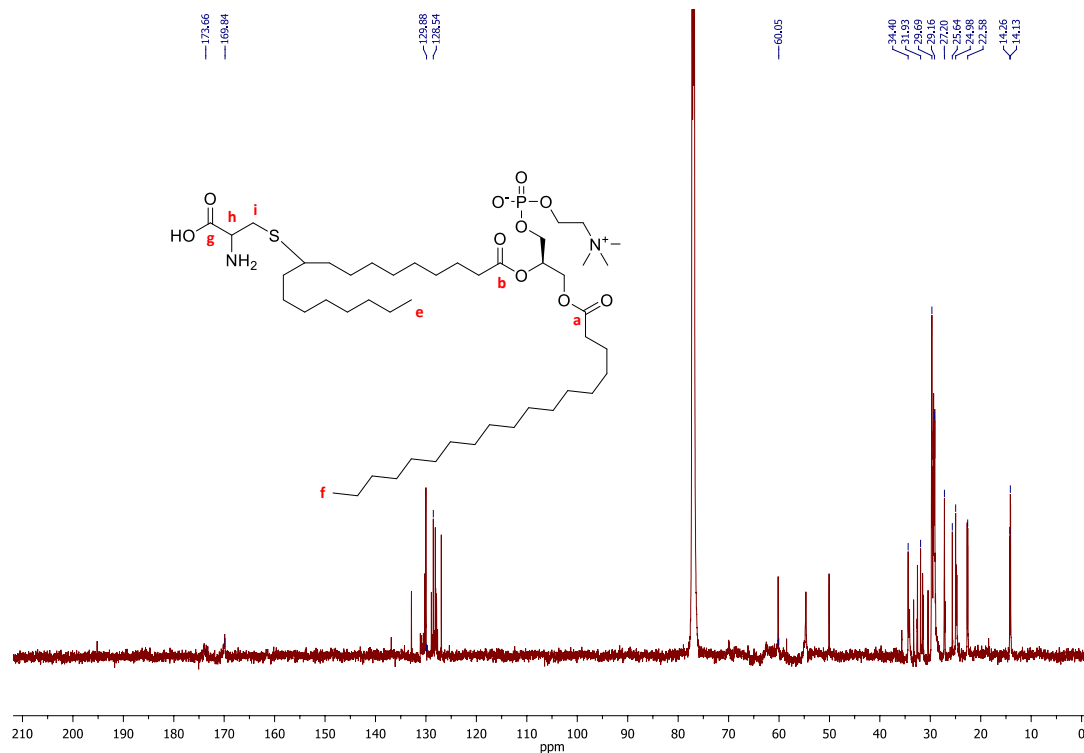


Fig. S8. ¹³C NMR spectrum of **Phos-Cys**.

¹³C NMR (150 MHz, CDCl₃, 25°C) **Phos-Cys**: δ 173 (–COO– **a** and **b**), 169.6 (–COOH cysteine **g**), 129 and 128 (remaining –CH=CH– from phosphatidylcholine), 60.0 (–CH– cysteine **h**), 34.4 (–CH₂– cysteine **i**), several singlets centred at 31.9, 29.7, 27.2, 25.6, 24.9, 22.5, and others (several phosphatidylcholine –CH₂– methylene groups), and 14.2 and 14.1 ppm (two terminal –CH₃ groups **e** and **f**).

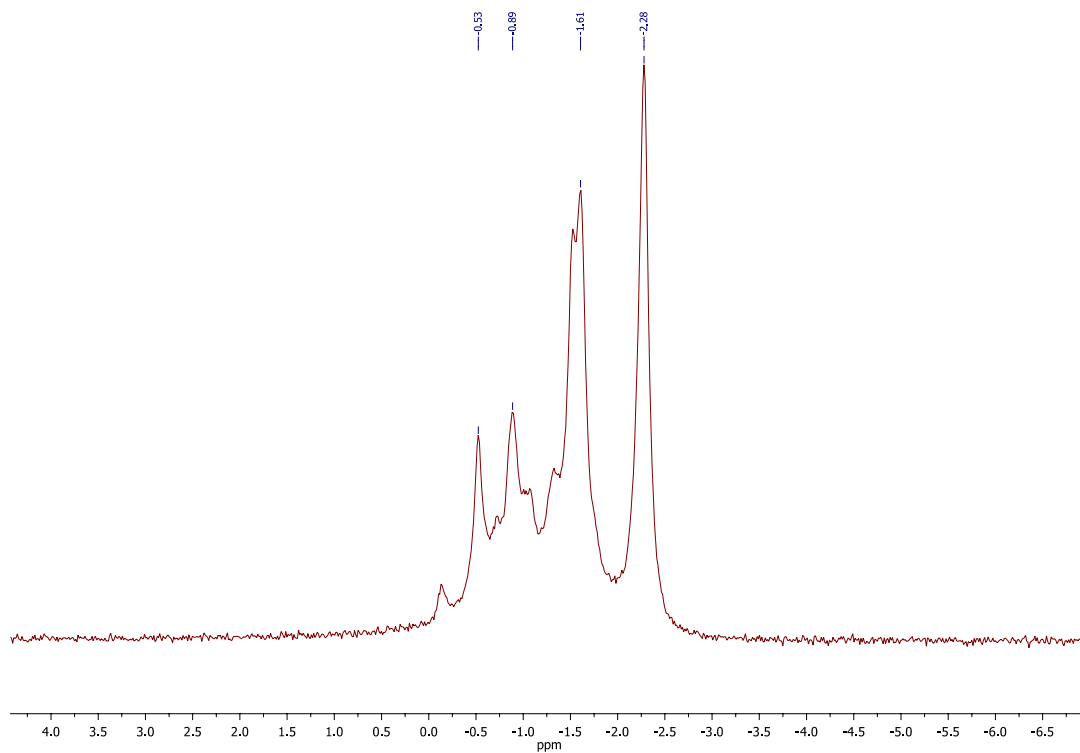


Fig. S9. ^{31}P NMR spectrum of **Phos-Cys**.

^{31}P NMR (173 MHz, CDCl_3 , 25°C) **Phos-Cys**: δ -2.3 s, and -1.52 s ppm. Smaller peaks at -0.9 and -0.5 ppm.

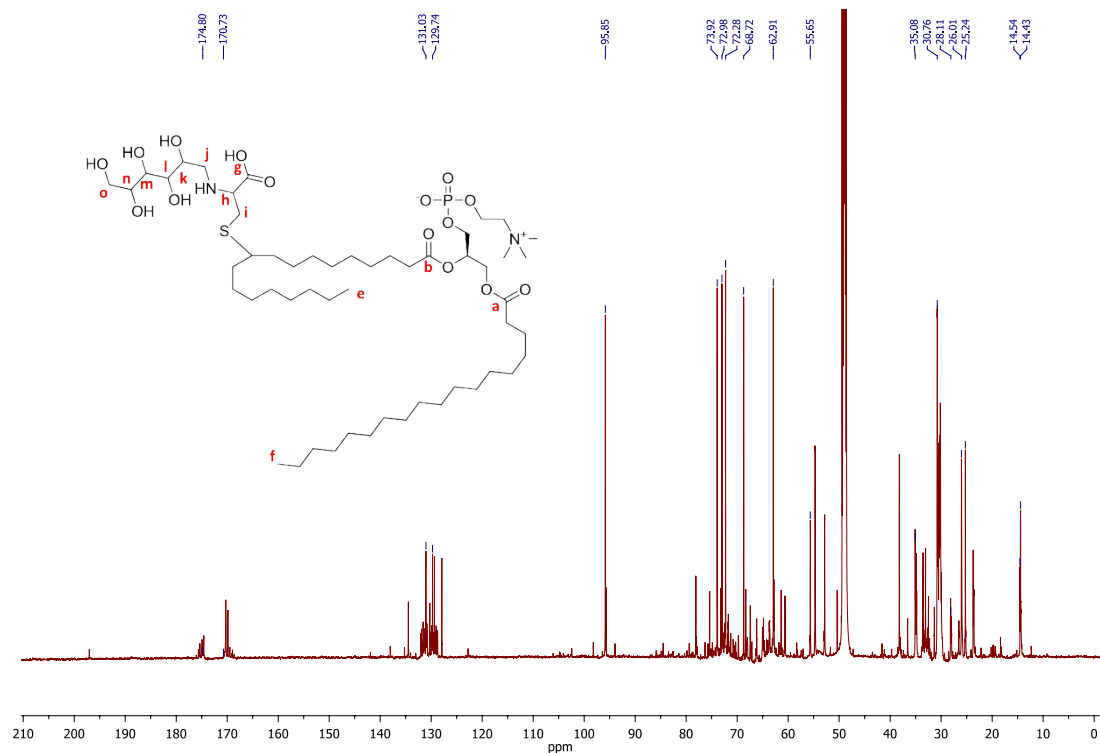


Fig. S10. ^{13}C NMR spectrum of **Phos-Cys-Man**.

^{13}C (150 MHz, MeOD, 25 °C) **Phos-Cys-Man**: δ 174 (–COO– **a** and **b**), 170.7 (–COOH cysteine **g**), 131 and 130 (residual –CH=CH–phosphatidylcholine), several singlets centred at 96.3, 74.4, 73.5, 72.8, 69.2 and 63.4 (D-mannose, **j**, **k**, **n**, **l**, **m** and **o**, respectively), 55.6 (–CH– cysteine **h**), 35.0 (–CH₂– cysteine **i**), singlets centred at 30.7, 28.1, 26.0, 25.2, and others (several phosphatidylcholine –CH₂– methylene groups), and 14.5 and 14.4 ppm (two terminal –CH₃ groups **e** and **f**).

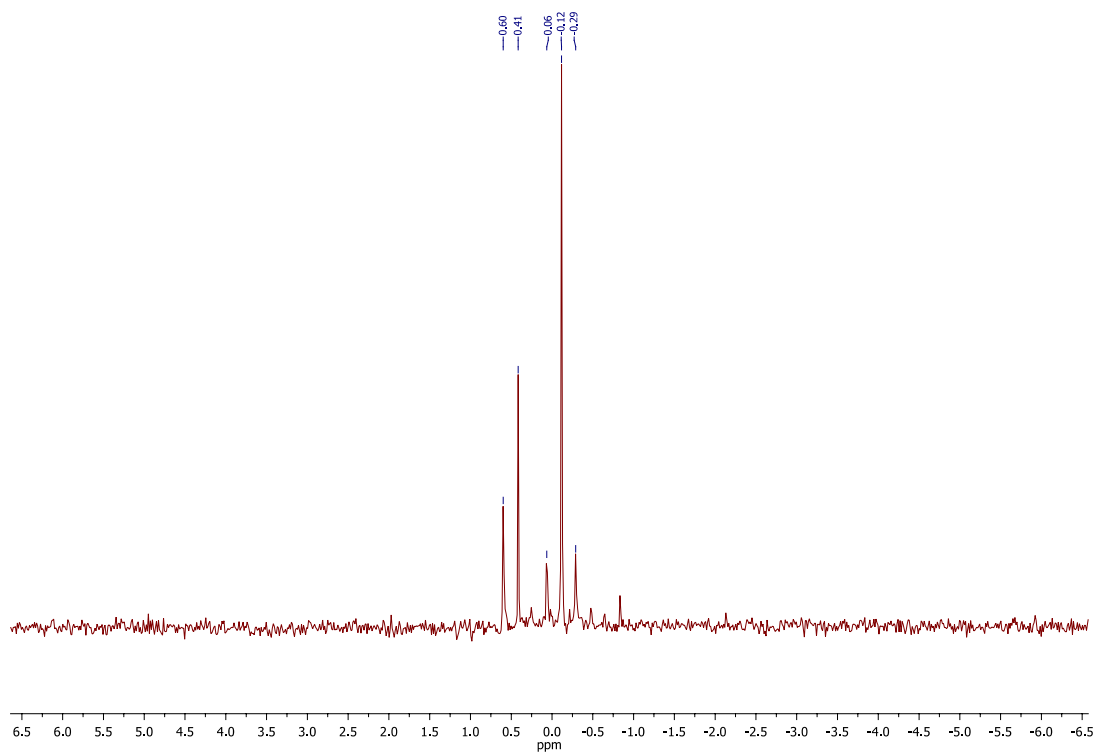


Fig. S11. ^{31}P NMR spectrum of **Phos-Cys-Man**.

^{31}P NMR (173 MHz, MeOD, 25°C) **Phos-Cys-Man**: δ -0.12 s, and 0.41 s ppm. Smaller peaks at 0.6, 0.06 and -0.29 ppm.

S7. Green metrics values

Table S5. Data used for the calculations of the green metrics with EATOS for the preparation of **Phos-Cys** (1st step).

	mol	g	Purity/Yield (%)	MW
L- α -Phosphatidylcholine	0.003	2.34	65	783
L-cysteine hydrochloride	0.003	0.36	98	121.15
Ethanol		20		
DMPA	0.0003	0.076	99	256
EtOH for wash		15		
Phos-Cys	0.0029	2.57	95%	

Table S6. Green metrics obtained with EATOS for the preparation of **Phos-Cys** (1st step).

	Contribution (%)			
	MI	E-factor	El_in	El-out
Auxiliaries	38.39	41.19	36.48	42.26
Solvents	51.19	54.93	48.64	56.34
Impurities	3.27	3.51	4.66	1.19
Catalyst	0.19		0.33	
Substrates	6.94		9.89	
By-products		0.14		0.05
Value (kg kg ⁻¹)	14.69	13.69	30.94	40.05

Table S7. Data used for the calculations of the green metrics with EATOS for the preparation of **Phos-Cys-Man** (2nd step).

	mol	g	Purity/Yield (%)	MW
Phos-Cys	0.0028	2.57	100	904
Mannose	0.0028	0.51	98	180.16
Ethanol		20		
EtOH for wash		20		
Product Phos-Cys-Mannose	0.0028	2.95	97%	
Coupled product (H ₂ O)	0.0028	0.05		

Table S8. Green metrics obtained with EATOS for the preparation of **Phos-Cys-Man** (2nd step).

	Contribution (%)			
	MI	E-factor	El_in	El-out
Auxiliaries	47.42	49.91	47.42	49.97
Solvents	47.42	49.91	47.42	49.97
Impurities				
Substrates	5.15		5.15	
By-products				
Coupled products		0.089		0.17
Value (kg kg ⁻¹)	19.93	18.94	59.82	56.76

Table S9. Green metrics obtained with EATOS for the preparation of **Phos-Cys-Man** considering a one-pot reaction.

	Contribution (%)			
	MI	E-factor	El_in	El-out
Auxiliaries	45.18	46.63	44.14	47.10
Solvents	50.19	51.81	49.05	52.34
Impurities	1.28	1.32	1.87	0.44
Substrates	3.274		4.79	
By-products				
Coupled products		0.05		0.02
Value (kg kg ⁻¹)	32.04	31.04	65.57	92.17

S8 Raman spectrometry

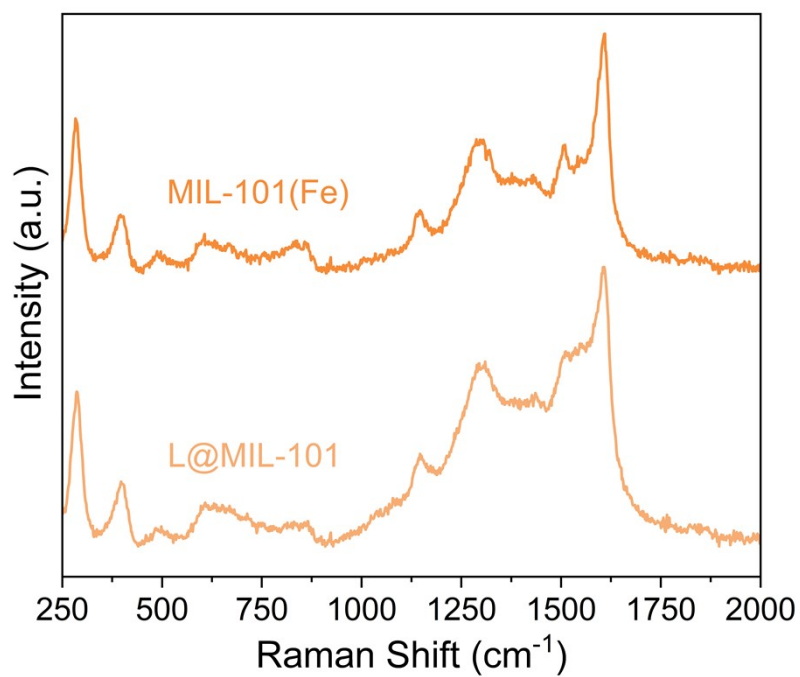


Fig. S12. Raman analysis of the pristine and functionalized MIL-101 (Fe) (“L@NPs”).

S9. DLS analysis

Table S10. Pdl values of the DLS measurements.

	MeOH	Pdl	H ₂ O	Pdl
PCN-222	155±52	0.092±0.03	161±39	0.22±0.03
UiO-66	1131±64	0.13±0.10	1129±146	0.10±0.09
MIL-101(Fe)	518±112	0.28±0.02	583±105	0.29±0.01
FeNPs	244±78	0.29±0.03	agglomerates	/
L@PCN-222	167±63	0.26±0.04	175±45	0.27±0.03
L@UiO-66	1198±133	0.12±0.08	1191±193	0.17±0.05
L@MIL-101(Fe)	540±55	0.28±0.02	530±133	0.14±0.03
L@FeNPs	287±91	0.29±0.03	299±101	0.19±0.09

S10. SEM images with mapping

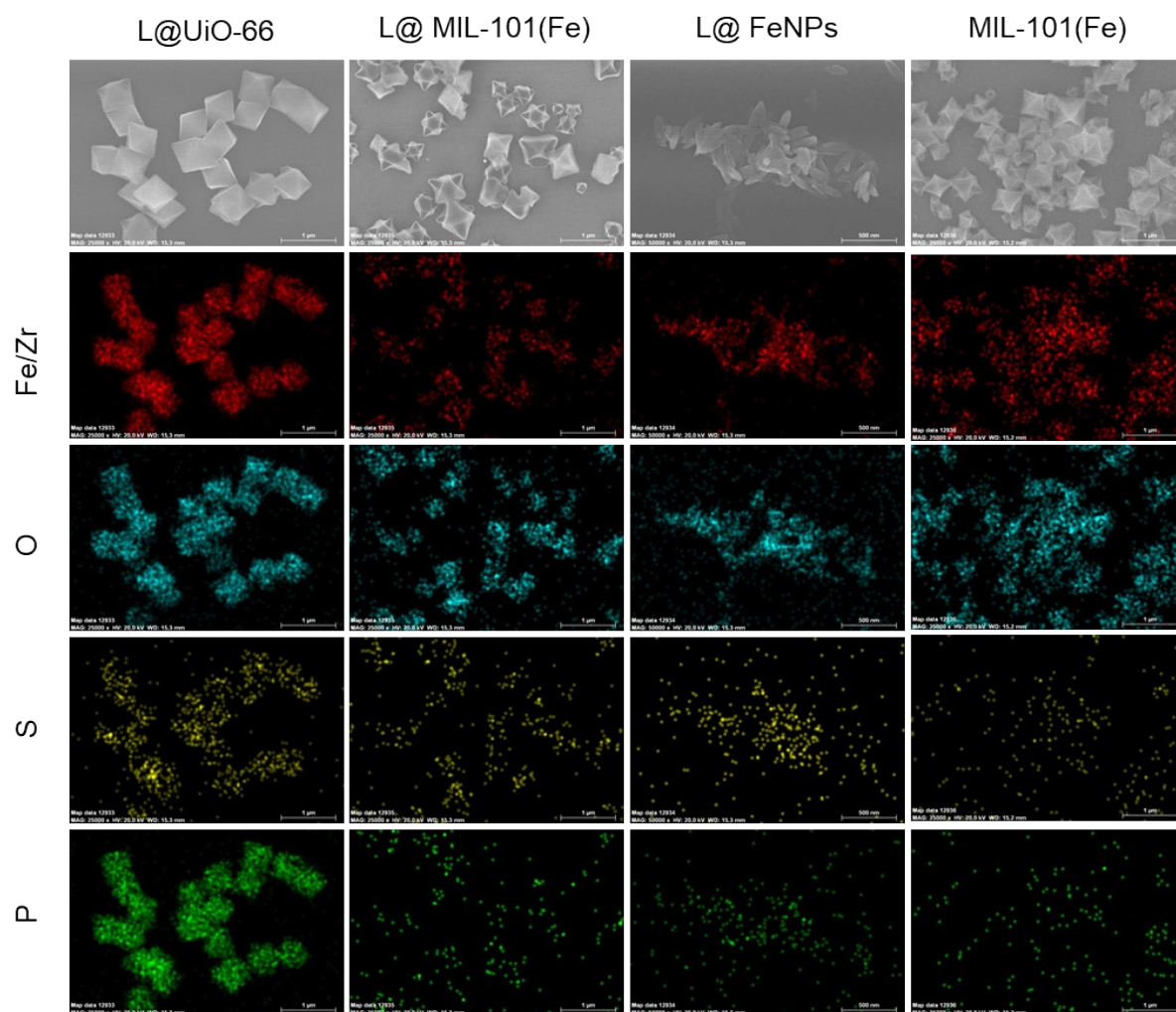


Fig. S13 . SEM images with mapping of iron (MIL-101(Fe) and FeNPs), zirconium (UiO-66), oxygen, sulfur and phosphorus.

S11. XPS analysis

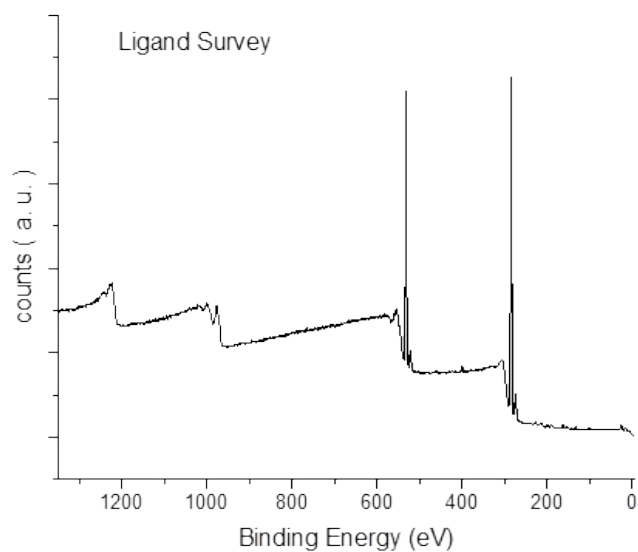


Fig. S14. XPS survey spectrum obtained for Pho-Cys-Man.

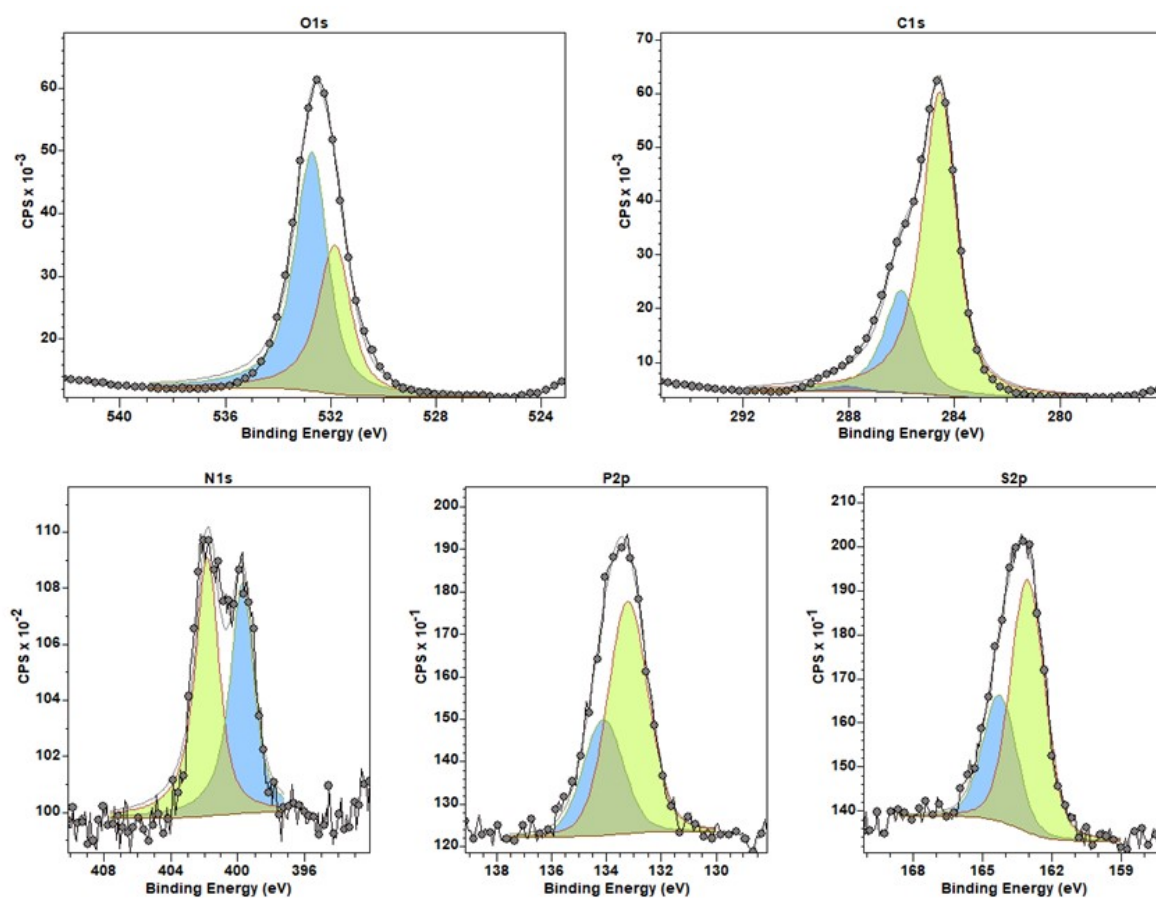


Fig. S15. XPS corresponding to C1s, O1s, N1s, P2p and S2p of Pho-Cys-Man.

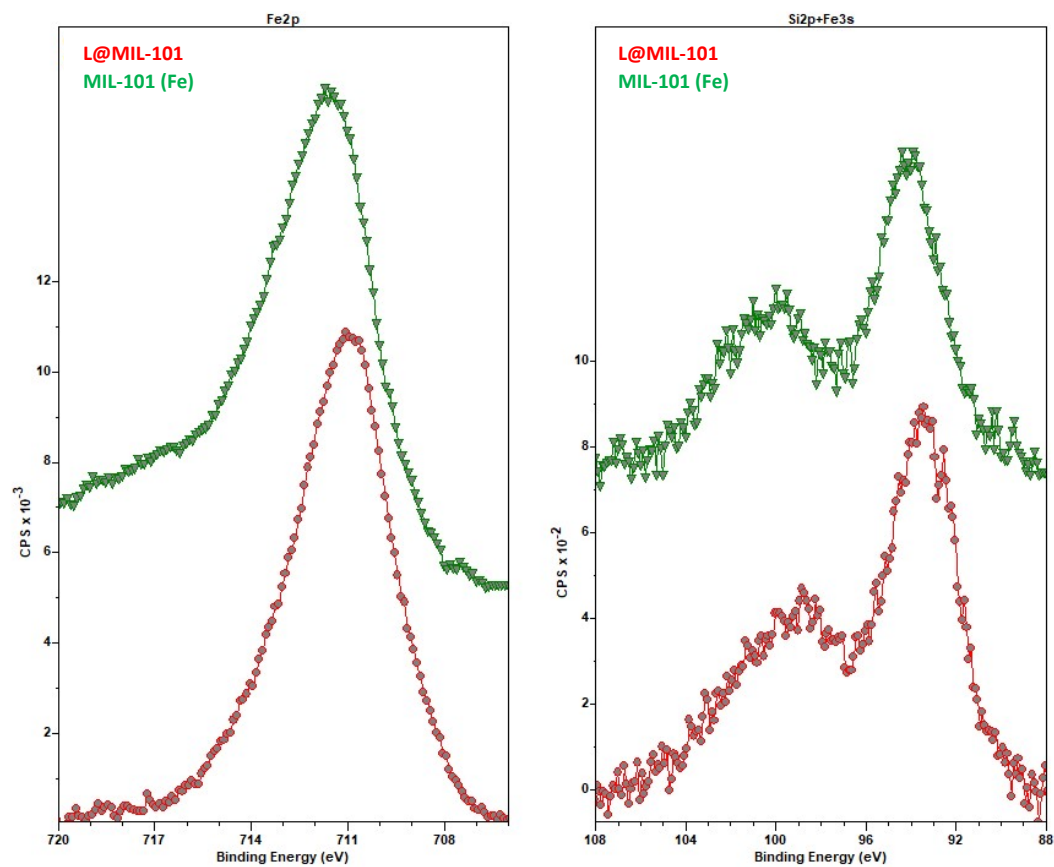


Fig. S16. XPS Fe2p (left) and Fe3s (right) spectra for MIL-101 (Fe) and L@MIL-101.

References

- 1 J. M. Orduña, N. del Río and M. J. Pérez-Pérez, *Org Biomol Chem*, 2023, **21**, 5457-5468.
- 2 A. Zuliani, M. Carmen Castillejos and N. Khiar, *Green Chem.*, 2023, **25**, 10596–10610.
- 3 D. Bůžek, S. Adamec, K. Lang and J. Demel, *Inorg Chem Front*, 2021, **8**, 720-734.
- 4 X. Fu, L. Jia, A. Wang, H. Cao, Z. Ling, C. Liu, E. Shi, Z. Wu, B. Li and J. Zhang, Zhang, *Icarus*, 2020, **336**, 113435.